THE INFLUENCE OF LANDER'S ROCKET JETS ON THE LUNAR SURFACE AT LANDING SITES: SMOOTHING OF ROUGHNESS OR MATURITY REDUCTION? Y. Shkuratov[1], V. Kaydash[1], G. Videen[2], [1]Karazin National University, 35 Sumska St, Kharkiv, 61022, Ukraine, [2]Space Science Institute, 4750 Walnut St. Suite 205, Boulder CO 80301, USA.

Introduction: The engine jets of lunar landers noticeably influence the lunar surface near landing sites (LS) at spacecraft descending/ascending [e.g., 1-8]. This manifests themselves as small areas that are a bit brighter than surroundings. To specificate this influence, other optical characteristics should be involved in analysis. For instance, these could be phase- or color-ratio imaging. The photometric phase-ratio method [10,11] has been applied to study structure variations of the lunar surface. In particular, this also allows investigations of spacecraft landing sites [2-7]. The investigations revealed the effect of scouring and smoothing of upper regolith layer caused by the impact of the gas jets from the rocket engines that destroy the primordial structure that effectively produces the shadow effect influencing the slope of phase curves.

The color-ratio technique allows us to assess the regolith maturity degree in LS, estimating the depths of gas jet influence on the surface [4]. Until recently, the smoothing by gas jets was considered dominant in their effect on the surface [2,4,5-7]. However, Yunzhao Wu and Bruce Hapke [8] now consider that the decreasing maturity of jet-influenced regolith is more important: *"brightness changes visible from orbit are related to the reduction in maturity due to the removal of the fine and weathered particles by the lander's rocket exhaust, not the smoothing of the surface"*. We here suggest several arguments, which support our initial interpretation exploiting the smoothing. We show that the factor maturity is secondary.

Data and Processing: For producing the phase-ratio and color-ratio images of the Apollo-15 LS, we here use, respectively, LRO NAC and Kaguya MultiImager (MI) data. The LRO NAC images have the highest spatial resolution near 0.5 m. The Kaguya MI data have the resolution of about 15 m that is much low than in the case of LRO NAC. However, because of the disturbed area around LS has the diameter of about 150 m, we may expect to resolve the landing site in color-ratio C(750/415 nm) and C(950/750 nm), where $C(\lambda_1/\lambda_2) = A(\lambda_1)/A(\lambda_2)$ and $A(\lambda)$ is the radiance factor [9]. We used the Kaguya MI image that is titled MI_MAP_03_N27E003N26E004SC. This is a mosaic after multispectral cube generation and map projection photometrically corrected to the standard RELAB geometry (i=30°, e=0°, and α =30°).

If there are images obtained at phase angles α_1 and α_2, their ratios $PR(\alpha_1/\alpha_2) = A(\alpha_1)/A(\alpha_2)$ can be calculated after their matching. We here study such a ratio for the Apollo-15 LS, considering $\alpha_1 > \alpha_2$. We used LRO NAC images of the site (M111571816L and M111578606L), which were acquired at $\alpha_2 = 30°$, $\alpha_1 = 55°$ and $\lambda_{eff} = 0.52$ μm. We omit a detailed description of the preparation procedure of C(750/415), C(950/750), and PR(55°/30°) images, referring to [11].

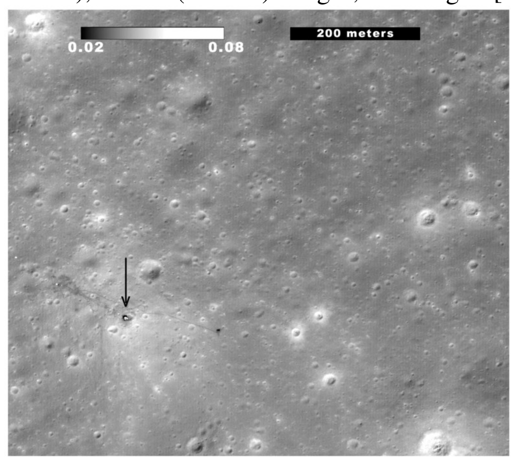

Figure 1. An image of Apollo-15 LS, presenting the radiance factor variations at α=30°

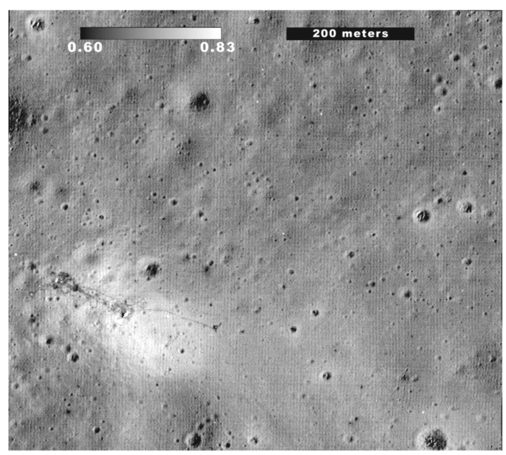

Figure 2. Ratio PR(55°/30°) for the scene seen in Fig. 1

Results and Discussion: Figure 1 shows the reflectance map comprising the Apollo-15 LS at α = 30°; the arrow indicates the lander. As can be seen, the area around the site is little bit brighter than surroundings, however, the effect is small and can be attributed to causes that do not related to the landing process. The area is clearly visible in the phase-ratio image shown in Fig. 2. There are no similar formations in the scene. We consider this area abnormally smoother than surroundings. A correlation diagram for *PR*(55º/30º) and *A*(30º) has been calculated (Fig. 3). The correlation coefficient is rather small, $k = 0.5$, but the diagram has a structure. In particular, the cluster in the ellipse corresponds to the Apollo-15 LS that is in accordance with its structure abnormality.

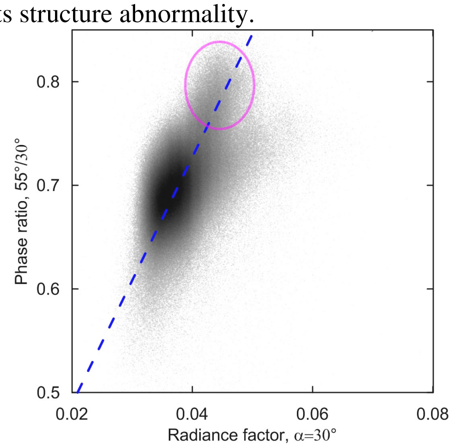

Figure 3. Correlation diagram *PR*(55º/30º) – *A*(30º) for the scene shown in Fig. 1. The ellipse outlines the cluster corresponding to the Apollo-15 LS. The central regression line is denoted with a dashed line

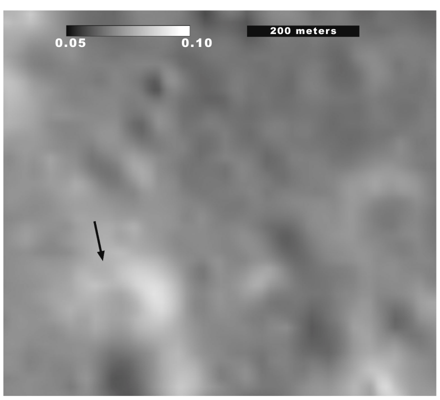

Figure 4. An image *A*(750 nm) of the Apollo-15 LS acquired with the Kaguya MI. The arrow indicates the position of the lander (also in Fig. 5 and 6).

Changes of the maturity degree due to the influence of gas jets of the lander rocket can be seen with Kaguya MI data, although they have much low surface resolution than LRO NAC data. Figure 4 shows an image *A*(750 nm) of the Apollo-15 LS acquired with Kaguya MI camera with resolution of about 15 m. The maturity degree is usually assessed using measurements of the color ratio *C*(950/750) [12-14]. The image shown in Fig. 5 does not reveal any anomaly in the site, whereas resolved young craters in the right bottom and upper left corners of the scene show low regolith maturity. The ratio *C*(750/415) also is sensitive to the maturity degree, however, Fig. 6 does not exhibit unusual behavior in the Apollo-15 LS and around, too.

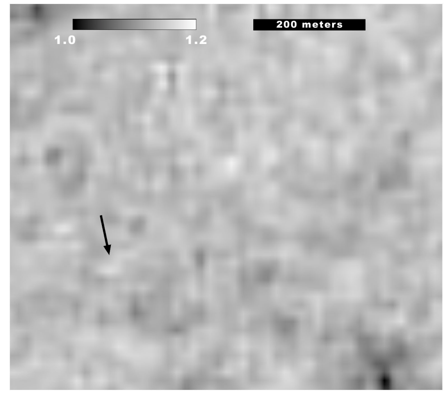

Figure 5. A color-ratio image *C*(950/750) of the Apollo-15 LS, which is built with data obtained with the Kaguya MI

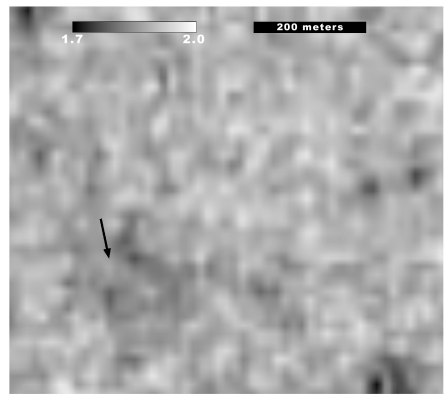

Figure 6. A color-ratio image *C*(750/415) of the Apollo-15 LS, which is built with data obtained with the Kaguya MI

Conclusion: We here present arguments that changes of the maturity degree in the Apollo-15 LS are rather faint. The same results have been obtained for Apollo-11 LS [4]. Thus, the albedo and phase-ratio variations in the Apollo LS probably are due to regolith structure changes that are caused by engine jets; the maturity degree produces a secondary effect.

References: [1] Metzger P. et al. (2011) *JGR, 116*, E06005, doi:10.1029/2010JE003745, [2] Kaydash V. et al. (2011) *Icarus 211,* 89–96. [3] Shkuratov Y. (2011) *PSS 59*, 1326-1371. [4] Kaydash V., Shkuratov Y. (2012) *Solar Syst. Res*. 46, 108-118. [5] Shkuratov Y. et al. (2013) *PSS 75,* 28–36. [6] Kaydash V. et al. (2013) *PSS 89,* 172–182. [7] Clegg R.N. et al. (2014). *Icarus 227*, 176–194. [8] Yunzhao Wu, Hapke B. (2018) *Earth and Planet. Sci. Let*. 484, 145–153. [9] Hapke B. (1993) *Theory of reflectance and emittance spectroscopy*, Cambridge Univ. Press, 450 p. [10] Shkuratov Y. et al. (1994) *Icarus 109,* 168-190. [11] Kaydash V. et al. (2012) *JQSRT 113*, 2601-2607. [12] Lucey P. et al (1995) *Science 268*, 1150-1153. [13] Lucey P. et al. (2000) *JGR 105(E8)*, 20,297–20,305. [14] Lucey P. et al. (2000) *JGR 105*, 20,377–20,386.